INTERNATIONAL JOURNAL OF MARITIME TECHNOLOGY

IJMT Vol.7/ Winter 2017 (29-37)

Available online at: http://ijmt.ir/browse.php?a_code=A-10-797-1&sid=1&slc_lang=en
DOI: 10.18869/acadpub.ijmt.7.29

Sandbar Migration Due to Cross-Shore Sediment Transport; A Case Study of Noshahr Coasts, Iran

Marzieh Hajiarab Derkani[1], Seyed Mostafa Siadatmousavi[2*], Seyed Masoud Mahmoudof[3]

[1] *Iran University of Science and Technology, Tehran, Iran; m_hajiarabderkani@alumni.iust.ac.ir*
[2] *Iran University of Science and Technology, Tehran, Iran; siadatmousavi@iust.ac.ir*
[3] *Iranian National Institute for Oceanography and Atmospheric Sciences, Tehran, Iran; m_mahmoudof@inio.ac.ir*

ARTICLE INFO

Article History:
Received: 5 Dec. 2016
Accepted: 15 Mar. 2017

Keywords:
Sediment transport
Sandbar
Wave
Current
Numerical modelling

ABSTRACT

Cross-shore sediment transport is one of the effective factors in erosion and sedimentation, and affects dynamics of the beach profile in coastal areas. Furthermore, sandbar migration due to cross-shore sediment transport mostly effects beach nourishment, displacement of pollutions trapped in sediments, and organism and plants' lives. In this manuscript, sandbar migration due to cross-shore sediment transport is studied and results have been compared to field data. Field data used here have been measured at the southern Caspian Sea, Noshahr coasts, Iran. During the measurement period, two high-energy events with significant wave height of approximately 1.4 m have been measured. All simulations have been done based on a one dimensional cross-shore transect. Wave transformation during propagation toward the coast has been modeled using the third generation model SWAN, and long-shore wave-induced current has been simulated by solving alongshore momentum equilibrium equation. To include the morphological change, the cross-shore sediment transport rate has been estimated using Bagnold [1966], Bowen [1980], and Bailard's [1981] (BBB) energetic sediment transport model, and results has been compared to the model developed by Plant et al. [2001], which itself is an energetic model based on Bagnold [1966]. Finally, bathymetric changes has been forecasted by solving cross-shore mass conservation equation which indicated slight outperform of BBB rather than Plant et al. model in this study area.

1. Introduction

Sandbars, of important properties of coastal morphological features, influence the nearshore wave and current regime and protect the coast against severe waves. Wave-induced currents, a result of wave breaking in surf zone, transport sediments and change morphological features of beaches. Predicting bathymetric evolution has been of interest in many previous studies by combining hydrodynamic models, a sediment transport model and an initial bathymetric observation whether from field experiments or laboratory wave tanks. For instance, Roelvink and Stive [9] have studied the role of cross-shore flow mechanisms, induced by random waves normally incident on a dissipative beach, in the two dimensional case of bar generation using laboratory data. This study concludes that however terms required by Bailard's [7] sediment transport model was accurately predicted by hydrodynamic model, onshore sediment transporting mechanisms were not accurately predicted by coupled hydrodynamic and sediment transport model, and suggested to implement a transport formulation which would use a near bottom flow property such as the asymmetry of the accelerations to include a non-instantaneous response. There are several studies that support this suggestion. For instance, Hoefel and Elgar [10] applied a dimensional form of acceleration skewness as a surrogate for the effects of acceleration in pitched forward waves, and reported an improved predictive skill of model, both for onshore and offshore bar migrations. Thornton et al. [11] and Gallagher at al. [12] assessed Bailard's [7] sediment transport model using field observation from Duck, North Carolina. These studies confirmed Roelvink and Stive's [9] results in which offshore transport associated with the advection by the cross-shore mean flow was predicted well, but the model underpredicted through

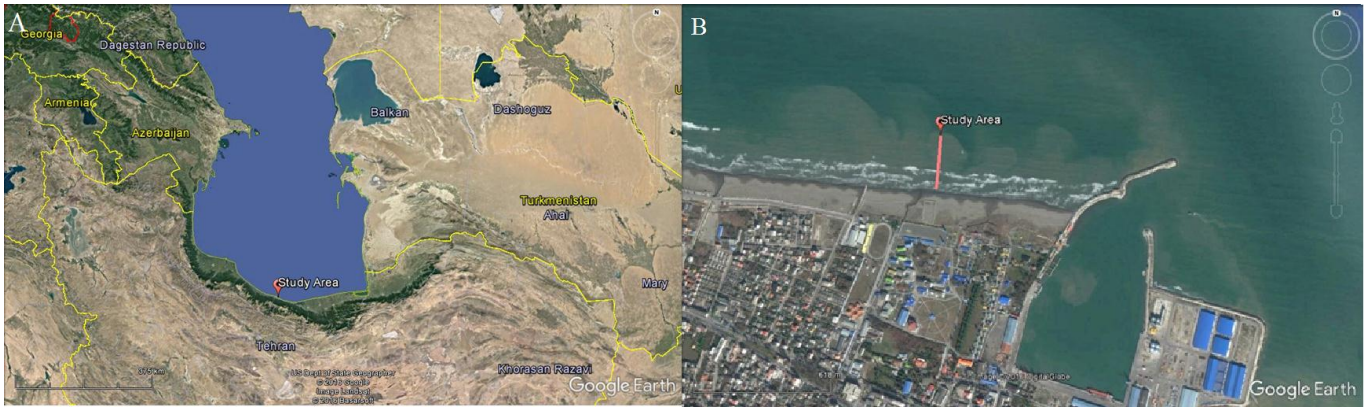

Figure 1. A) Southern Caspian Sea, B) Noshahr port and the location of study area.

development. For making accurate transport predictions, Thornton et al. [11] suggested to include the alongshore current which was contributing in stirring of sediment. Reasonable model predictions during storms were consistent with Bagnold's [5] sediment transport model based on unidirectional flow in a river. It is hypothesized that stream flow resembled by strong longshore current has in part caused the good agreement. Gallagher et al. [12] suggested the inclusion of cross-shore varying fall velocity that can improve model performance, and supposed that as the model does not include the effects of fluid acceleration nor the effects of phase lags between fluid and sediment, both of which may be important when oscillatory wave velocities dominate the flow, the onshore bar migration was not predicted properly.

Plant at al. [8] have considered the morphological implications associated with Bagnold's [5] sediment transport model by factoring it into a dimensional and none dimensional transport terms.

They concluded that the combined influences of mean flow, flow-sediment correlation and slope can be well modelled with a polynomial dependence on the relative wave height and linear beach slope dependence.

The purpose of this paper is to predict sandbar migration due to cross-shore sediment transport using BBB and Plant et al.'s [8] sediment transport models, and compare the results with observations. Section 2 consists of the dataset used for testing the models' performance. Hydrodynamic, sediment transport and bathymetric prediction methods are described in section 3. Then model results, and evaluation of their skills are presented in section 4. The conclusion in section 5 summarizes these findings.

2. Observations

A series of field measurements have been carried out at the west of Noshahr port, southern Caspian Sea coasts (Figure 1). The measurements have been conducted from March 3rd to 16th, 2014. The bathymetry survey was performed at the beginning and the end of data recording. The water level fluctuations have been recorded using 4 pressure sensors stations located at surf zone from the depth of 4.8 m at the offshore station to 1.3 m near the shore line. All stations were placed along a shore perpendicular transect shown in figure 1-B. Considering the location of the study area, longshore sediment transport might affect sedimentation processes. Regarding the short time of this study, this minor effect has been ignored.

The bathymetry surveys at March 3rd and 16th and the station locations are also presented in Figure 2. As can be seen in this Figure, beach profile changes have been small enough to ignore the depth change in the wave model and use the initial bathymetry in the wave model for entire period of the simulation.

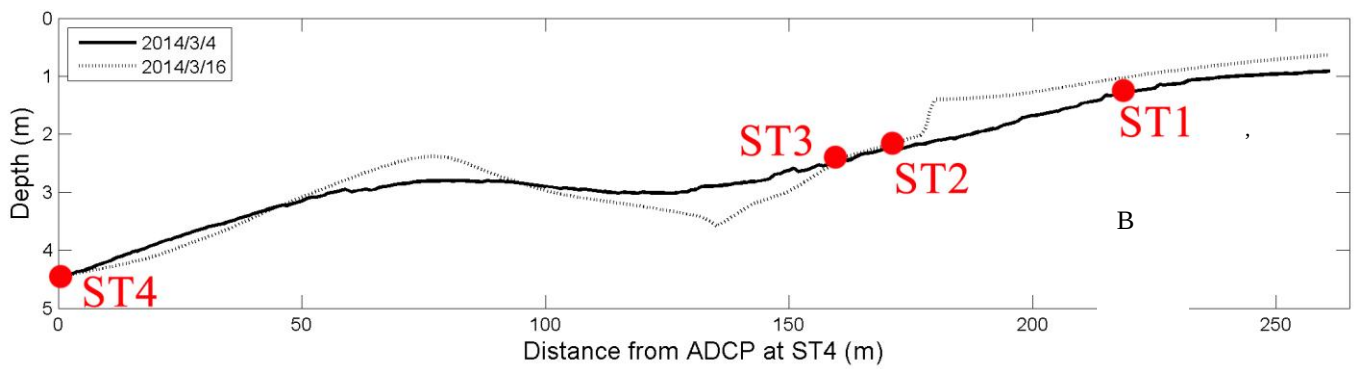

Figure 2. Beach profile changes and measurement stations distribution.

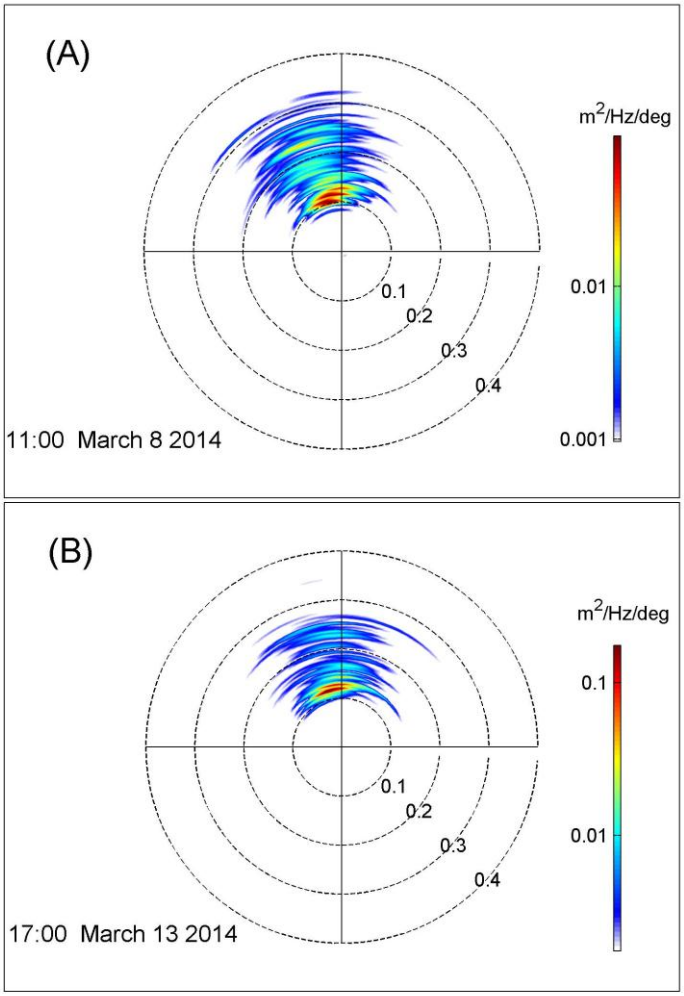

Figure 3. A) Wave full energy density distribution at 11:00 o'clock March 8th, 2014, B) Wave full energy density distribution at 17:00 o'clock March 13th, 2014.

Time series of current profiles and the incident wave spectrum have been measured continuously using a 600 KHz upward-looking RDI ADCP at the outer surf zone station (ST4, 310 m far from shoreline), with data acquisition rate of 2 Hz, which was set to record 20 minutes averaged velocity within each hour at 25 cm bins. There has been no significant current, unless wave driven currents, at the study area in the period of observations. The hourly averaged current intensities have been 0.09 m/s and 0.02 m/s in the longshore and cross-shore direction respectively [13] (for more information about instrumentation please refer to [13]).

Two high-energy events have been occurred during the measurement period with maximum significant wave height of about 1.4 m and peak period of 9.5 s, lasting for 11 and 18 hours respectively. These non-locally generated young swells arrived from distant sources, from the central part of the Caspian Sea, approximately 600 km away from the study area. The predominant incident wave direction has been normal to the shore altering about 4 degrees. Wave full energy density distribution is depicted in Figure 3 for two sample dates during the first and second high-energy events.

Wind speed was negligible during this time period and $V_{10} = 6\,^{m}/_{s}$ was recorded at a coastal synoptic station located 10 km west of the study area. The tide is negligible and the water level oscillation of less than 10 cm has been recorded.

3. Methods

3.1. Wave Transformation

One dimensional wave transformation on the shore perpendicular transect from ADCP location to the coastline was simulated using SWAN 1D model developed at Delft University of Technology [14].

This third-generation wave model solves the wave action balance equation (valid at the presence of currents [15]) with sources and sinks. The wave action (N) is defined as:

$$N \equiv E / \sigma \tag{1}$$

where E and σ denote wave energy and relative frequency respectively. The wave propagation is described as following:

$$\frac{\mathrm{DN}}{\mathrm{Dt}} = \frac{S}{\sigma} \tag{2}$$

in this equation, *DN/Dt* represents the total time derivative and *S* is composed of any energy source or sink.

In deep water, *S* is primarily determined by wind-energy input, quadruplet wave-wave interaction, and white capping dissipation; whereas in intermediate and shallow water, depth-induced wave breaking, bed friction and triad wave-wave interaction effects might significantly control the shape of the wave spectrum.

In this study, the quadruplet wave-wave interaction has been neglected (regarding the negligible wind speed and short spatial scale of the study area), and the wave energy dissipation resulted from depth-induced wave breaking has been considered using the formula presented by Thornton and Guza [16]. A time step of 10 seconds and a grid spacing of 10 m were used in wave transformation computations.

3.2. Wave-Driven Currents

The mean alongshore current is computed assuming a balance between the alongshore component of cross-shore energy flux gradient and a current-opposing bottom stress [3, 11]. The alongshore current is found by solving an alongshore momentum balance [4].

$$-\frac{\sin[\theta(x,\bar{t})]}{\rho c(x,\bar{t})} D_r(x,t) + \mu \frac{\partial}{\partial x}[d(x)\frac{\partial}{\partial x}\bar{v}(x,t)] = c_f[\bar{v}^2(x,t) + \alpha^2\sigma_u^2(x,t)]^{1/2}\bar{v}(x,t) \quad (3)$$

where c is the local wave celerity, c_f is an empirical drag coefficient (assumed to be a constant), α is correction parameter associated with the correlation between alongshore and cross-shore components of the instantaneous velocity field [1] (suggested as α = 1.16 as an optimum value), and μ is an empirical eddy diffusion coefficient, which is an adjustable parameter [4].

Here, c_f has been calculated using the following equation [17]:

$$c_f = 0.015\left(\frac{k_a}{h}\right)^{1/3} \quad (3a)$$

in which, k_a is the bed roughness and h is the water depth.

The roller energy dissipation is used as forcing. The roller energy (E_r) and its dissipation (D_r) are computed as:

$$D_r(x,t) = 2gE_r(x,t)\beta / c(x,t) \quad (3b)$$

$$\frac{\partial}{\partial x}[2c(x,t)\cos\theta(x,t)E_r(x,t)] = D_w(x,t) - D_r(x,t) \quad (3c)$$

where β was set to 0.1 as a standard value [4,18]. The wave energy dissipation rate, D_w, is described as following [3]:

$$D_w(x,t) = \frac{3\rho g B^3 \gamma^2 \sqrt{\pi} f}{16} H_{rms}^2(x,t)\Gamma^3(x,t) .\{1-[1+{\Gamma^2(x,t)}/{\gamma^2}]^{-\frac{5}{2}}\} \quad (4)$$

where B is a description of breaking wave geometry, Γ and γ are the normalized wave height and its critical value, and f is the peak frequency of the incident waves. The parameters B and γ are typically used to tune the wave model to give optimum estimates of the wave height, and here they were set to 1.0 and 0.36 [2,18]. Because of their strong nonlinear dependencies, each of the formulations in equations (3) and (4) must be solved numerically. Equation (3) is a second-order ordinary differential equation, which requires specification of two boundary conditions for $\bar{v}$ (or its gradients). We assumed $\bar{v}(shore,t) = 0$ and $\frac{\partial}{\partial x}\bar{v}(sea,t) = 0$, and equation (3c) is a first-order ordinary differential equation, and is solved with a simple forward stepping scheme. Grid spacing of 1 m has been deployed in these solutions assuming stationary condition in each hour. As wave transformation grid spacing has been 10 m, the wave height and period were linearly interpolated between grids.

3.3. Bed Evolution and Sediment Transport

3.3.1. BBB Sediment Transport Model

Energetic models based on Bagnold's [5] theory for bedload transport in unidirectional flows, have been extended to unsteady nearshore flows by relating the sediment transport rate to moments of the near bed flow velocity [6, 7]. The Bagnold/Bowen/Bailard (BBB) model can be written as following:

$$\langle\vec{i}\rangle = k_b\left\{\left\langle|\vec{u_t}|^2\vec{u_t}\right\rangle - \frac{\tan\beta}{\tan\phi}\left\langle|\vec{u_t}|^3\right\rangle.\hat{i}\right\} + k_s\left\{\left\langle|\vec{u_t}|^3\vec{u_t}\right\rangle - \frac{\varepsilon_s}{w_s}\tan\beta\left\langle|\vec{u_t}|^5\right\rangle.\hat{i}\right\} \quad (5a)$$

in which, k_b and k_s are defined as:

$$k_b = \rho\frac{c_f\varepsilon_b}{\tan\phi} \quad (5b)$$

$$k_s = \rho\frac{c_f\varepsilon_s}{w_s} \quad (5c)$$

in equation (5), β is the bed slope angle of the coastal profile, ϕ is the friction angle, ε_s and ε_b are suspended and bedload efficiency coefficients respectively, w_s is

the settling velocity of sediment particles, ρ is the water density, c_f is the drag coefficient, and total near bed velocity ($\overrightarrow{u_t}$, consisting of longshore and cross-shore components), is calculated as following:

$$\vec{u}_t = \vec{\tilde{u}} + \vec{\bar{u}} \tag{5d}$$

in this equation $\vec{\tilde{u}}$ and $\vec{\bar{u}}$ represent fluctuating and mean velocity respectively.

3.3.2. Plant et al.'s [8] Sediment Transport Model

This model intends to add to the theoretical discussions of Bowen [6] and Bailard [7], and others on the morphological implications of Bagnold's [5] sediment transport model. Time-averaged sediment transport is described as following in this model:

$$\overline{Q} = c_2 \frac{1}{16\sqrt{2}} \frac{\rho\sqrt{g}}{\tan\phi} H_{rms}^3 h^{-3/2} \cdot \left\{ -\left(\frac{1+c_1\sqrt{2}}{\sqrt{2}} \right) .y + c_2 \left(\frac{2}{\sqrt{\pi}} \frac{\tan\beta}{\tan\phi} + R_{su}^{other} \right) \right\} \tag{6a}$$

where ϕ is the angle of repose of sediment particles, h is the water depth, β is the beach slope, and R_{su}^{other} is described as:

$$R_{su}^{other} \approx \psi / \sqrt{2} \tag{6b}$$

in which ψ is the normalized velocity skewness:

$$\psi = \frac{\overline{(u-\bar{u})^3}}{\sigma_u^3} \tag{6c}$$

where c_1 is a constant of *O(1)*, and c_2 is described as:

$$c_2 = C_f' (\rho_s - \rho) / \rho_s \tag{6d}$$

where ρ and ρ_s are water and sediment density, and $\acute{C}_f$ is:

$$C_f' = \varepsilon C_f \tag{6e}$$

in which C_f is the friction factor and ε is the Bagnold's transport efficiency factor.

3.3.3. Bed Evolution

Assuming there are no longshore gradients in longshore sediment flux, mass conservation in the cross-shore direction yields:

$$(1-p)\frac{dh}{dt} = \frac{dQ(x)}{dx} \tag{7}$$

where $\frac{dh}{dt}$ is the change in bed elevation h with time t, and p is the bed porosity, supposed 0.3 in this study.

3.4. Prediction Skill

Models performances are assessed using Root Mean Square Error (RMSE) and Brier Skill Score (BSS) to provide an objective measure to model skill, defined as:

$$\mathrm{RMSE} = \sqrt{\frac{\sum_{n=1}^{N} (\hat{\theta} - \theta)^2}{N}} \tag{8}$$

where $\hat{\theta}$ and θ are observed and estimated changes in N measurement points, and:

$$\mathrm{BSS} = 1 - \frac{\langle (z_m - z_c)^2 \rangle}{\langle (z_0 - z_m)^2 \rangle} \tag{9}$$

Brier skill score compares the mean square difference between the calculated prediction, z_c, and the measured change, z_m, with mean square difference between the initial condition, z_0, and measured change. Perfect agreement gives a Brier score of 1, whereas modelling the baseline condition gives a Brier score of 0. Van Rijn et al. [19] provides a strict set of qualifications based
on BSS (1<BSS<0.8 = excellent, 0.8<BSS<0.6 = good, 0.6<BSS<0.3 = reasonable, 0.3<BSS<0 = poor and BSS<0 = bad).

4. Results and Discussion

Wave model has been calibrated using gamma, defined as proportion of root mean square breaker wave height to the water depth, and gamma=0.41 has been chosen as the best fit, the same as value reported by Thornton and Guza's [16] study. Figure 4 designates comparison between modelled and observed significant wave height in measurement stations. Average RMSE in measurement stations are 0.20, 0.18, 0.16, 0.15, 0.14 and 0.13 for gamma values equal to 0.3, 0.33, 0.36, 0.39, 0.42 and 0.45. As can be seen in Figure 4-D, predictions are not successful enough at ST1 due to the lack of model precision where wave breaking condition is dominant. By omitting ST1, average RMSE in measurement stations will reduce to 0.16, 0.14, 0.12, 0.10, 0.09 and 0.08 for gamma values equal to 0.3, 0.33, 0.36, 0.39, 0.42 and 0.45, hence further simulations are restricted to ST4-ST2.

In ST4 the open boundary information is provided, as a result, observations and predictions are so similar in this station, and little differences are because the model only accounts waves which are entering the domain of study and not those exiting it.

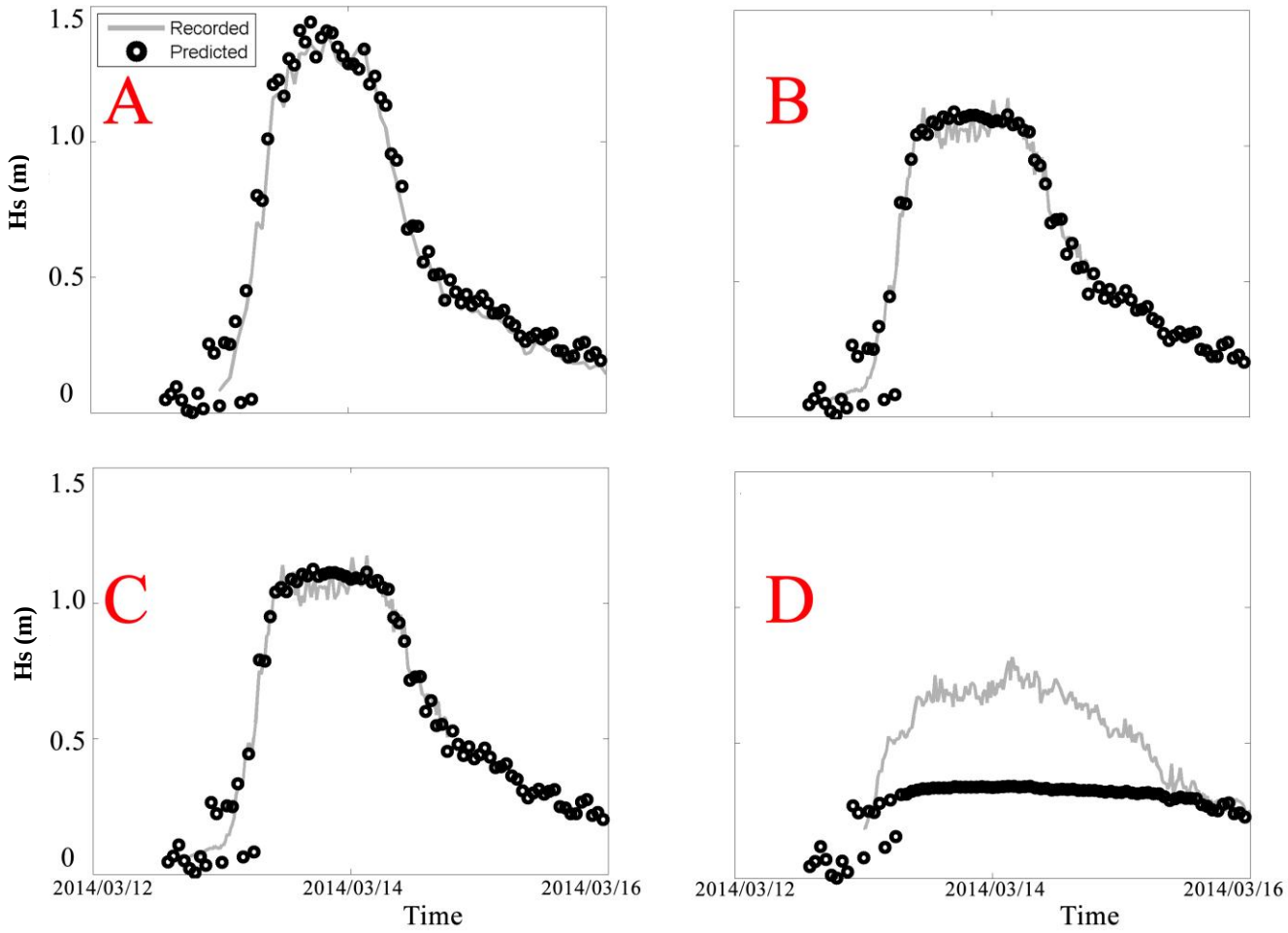

Figure 4. Comparison between modelled and observed significant wave height (Hs), ST4, B) ST3, C) ST2, D) ST1

Wave-driven current simulation results at ST4 are shown in Figure 5. Models adopted here predict current velocities with reasonable skill during high-energy events (in which major bed changes are expected to happen) with root mean square error equal to 0.077 and 0.068 m/s and correlation coefficient equal to 0.81 and 0.83 (Figure 6). Maximum standard deviation of wave-induced current velocity in depth has been 0.10 m/s and 0.11 m/s, and maximum standard deviation of current direction in depth has been 16.5 degree and 18.6 degree during the first and second high-energy conditions respectively. Considering the negligible current velocity and direction standard deviations, applying depth averaged models adopted here is reasonable.

Figure 7 depicts models predictions of bed elevation changes on the shore perpendicular transect, and its comparison to bathymetry observations before and after high-energy events. In these predictions, BBB and Plant et al.'s [8] sediment transport models are used, and their predicting skills are compared in Table 1. Based on BSS, the models' performance were reasonable; although BBB model slightly outperformed the Plant et al [8].

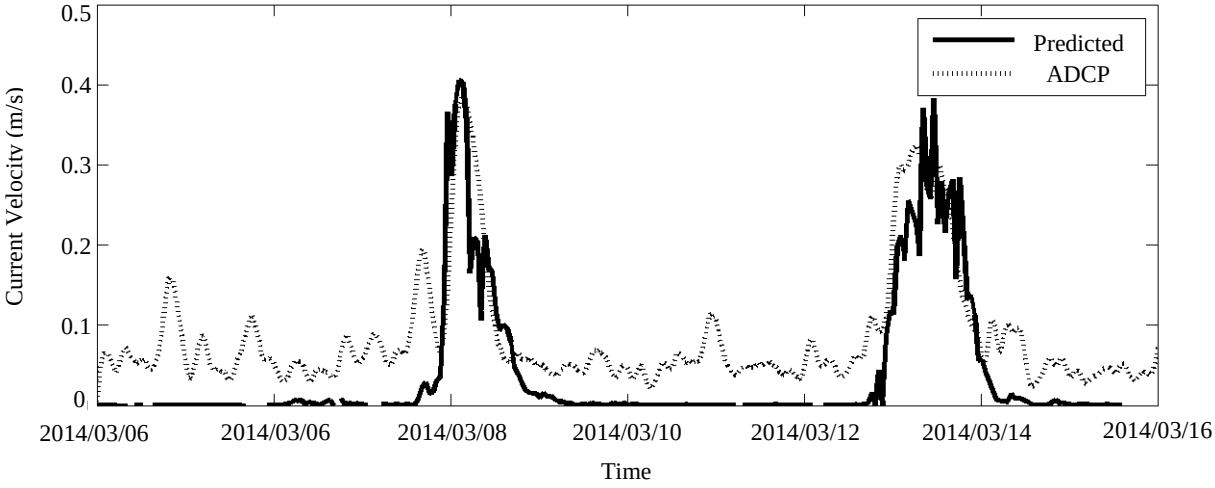

Figure 5. Comparison between modelled and observed vertically-averaged current velocity at ST4

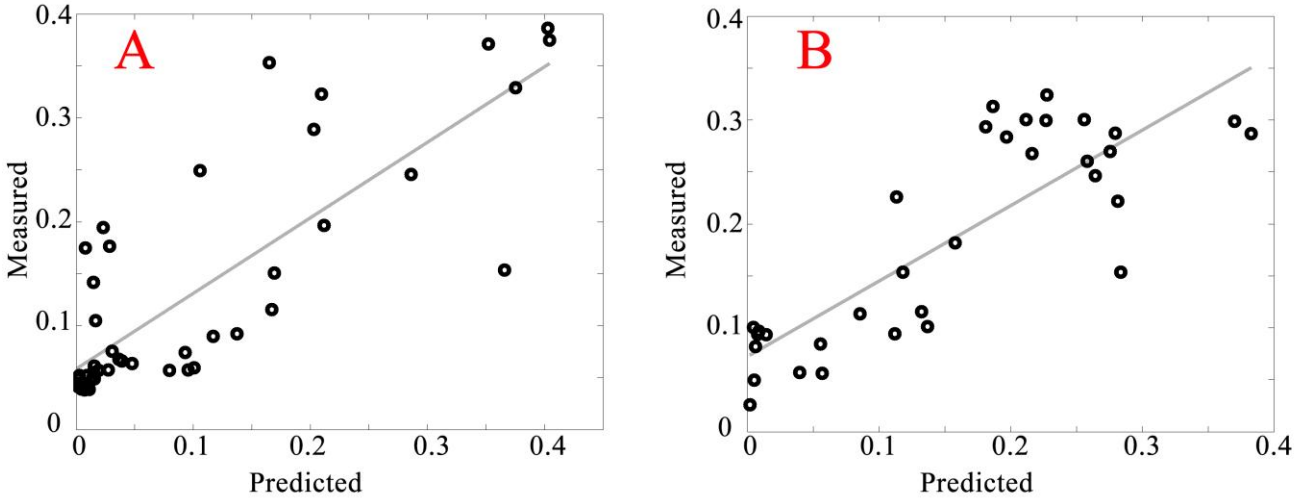

Figure 6. A) Scatter plot of modelled and observed current velocity during the first high-energy event, B) Scatter plot of modelled and observed current velocity during the second high-energy event.

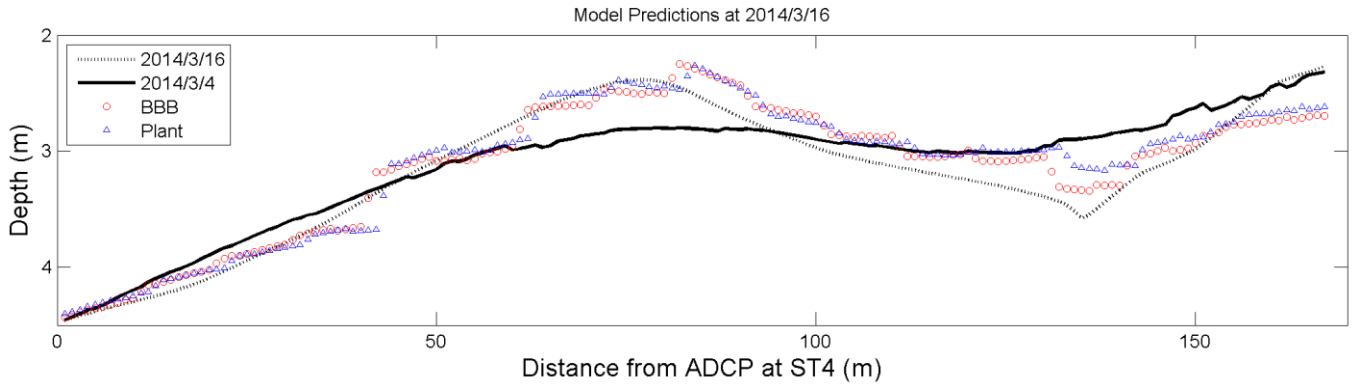

Figure 7. Prediction of bed elevation changes using BBB and Plant et al.'s sediment transport model

Table 1. BBB and Plant et al.'s [8] sediment transport model skills

RMSE (m)		BSS (dimentionless)	
BBB	Plant (2001)	BBB	Plant(2001)
0.1685	0.1889	0.4665	0.4659

5. Conclusion

In this study, sandbar migration due to cross-shore sediment transport has been investigated and results have been compared to field data. Field data used here have been measured during winter in a thirteen day period, at Noshahr coasts, Iran. They include hydrodynamic parameters, bathymetric data, and bed sediment samples.

One dimensional cross-shore transect has been simulated for wave, current, sediment transport and bed level change. Significant wave height (Hs) has been modelled using SWAN 1D model with average root mean square error of 0.09 m between stations located in the depth of 4.7 m to 2.2 m. Longshore wave-induced current has been numerically solved using the alongshore momentum equilibrium equation. The root mean square errors of modelled longshore current velocity are 0.077 and 0.068 m/s during the first and second high-energy events occurred during data casting at ST4, respectively.

At last, cross-shore sediment transport rate has been estimated using Bagnold [5], Bowen [6], and Bailard's [7] energetic sediment transport model (BBB), and results has been compared to the model used in Plant et al. [8], which itself is an energetic model based on Bagnold [5]. Afterward bathymetric changes have been forecasted by solving cross-shore mass conservation equation.

Root mean square error of modelling bathymetric changes using BBB model for sediment transport is approximately 0.17 m. The corresponding value for Plant et al.'s [8] model is 0.19 m. Narrowly we can say that BBB model has been more successful in estimating the sediment transport rate compared to the model used in Plant at al. [8].

BBB and Plant et al.'s [8] models, both among modern energetic sediment transport models, have been compared in this paper. These models are quite more successful than commonly used engineering models like Bijker [20]; however, optimized model can be found for any region by simulating the area using the models adopted here.

7. References

1- Feddersen, F., Guza, R. T., Elgar, S., & Herbers, T. H. C. (2000), *Velocity moments in alongshore bottom stress parameterizations*, Journal of Geophysical Research: Oceans, 105(C4), 8673-8686.

2- Haines, John W, and Asbury H Sallenger. (1994), *Vertical structure of mean cross-shore currents across a barred surf zone*, Journal of Geophysical Research: Oceans, 99: 14223-42.

3- Longuet-Higgins, Michael S. (1970), *Longshore currents generated by obliquely incident sea waves: 1*, Journal of geophysical research, 75: 6778-89.

4- Ruessink, BG, JR Miles, F Feddersen, RT Guza, and Steve Elgar. (2001), *Modeling the alongshore current on barred beaches*, Journal of geophysical research, 106: 22451-63.

5- Bagnold, RA. (1966), *An approach to the sediment transport problem*, General Physics Geological Survey, Prof. paper.

6- Bowen, A.J.. (1980), *Simple models of nearshore sedimentation; beach profiles and longshore bars*, Geological Survey of Canada: 1-11.

7- Bailard, James A. (1981), *An energetics total load sediment transport model for a plane sloping beach*, Journal of Geophysical Research: Oceans, 86: 10938-54.

8- Plant, NG, BG Ruessink, and KM Wijnberg. (2001), *Morphologic properties derived from a simple cross-shore sediment transport model*, JOURNAL OF GEOPHYSICAL RESEARCH-ALL SERIES-, 106: 945-58.

9- Roelvink, J.A. and Stive, M.J.F., (1989), *Bar-generating cross-shore flow mechanisms on a beach Barre* provoquant des mecanismes d'ecoulement perpendiculaires a la plage. J Geophys Res C Oceans 94 (4), 4785-4800.

10- Hoefel, Fernanda, and Steve Elgar. (2003), *Wave-induced sediment transport and sandbar migration*, Science, 299: 1885-87.

11- Thornton, EB, RT Humiston, and W Birkemeier. (1996), *Bar/trough generation on a natural beach*, Journal of Geophysical Research: Oceans, 101: 12097-110.

12- Gallagher, Edith L, Steve Elgar, and RT Guza. (1998), *Observations of sand bar evolution on a natural beach*, Journal of Geophysical Research: Oceans, 103: 3203-15.

13- Mahmoudof, S.M., Badiei, P., Siadatmousavi, S.M. and Chegini, V., (2016), *Observing and estimating of intensive triad interaction occurrence in very shallow water*. Continental Shelf Research, 122, pp.68-76.

14- Booij, N, RC Ris, and Leo H Holthuijsen. (1999), *A third-generation wave model for coastal regions: 1. Model description and validatio'*, Journal of Geophysical Research: Oceans, 104: 7649-66.

15- Whitham, G.B., (1965), *A general approach to linear and non-linear dispersive waves using a Lagrangian.* Journal of Fluid Mechanics, 22(02), pp.273-283.

16- Thornton, E.B. and Guza, R.T., (1983), *Transformation of wave height distribution*, Journal of Geophysical Research: Oceans, 88(C10), pp.5925-5938.

17- Sleath, John FA. (1984), *Sea bed mechanics.*

18- Lippmann, TC, AH Brookins, and EB Thornton. (1996), *Wave energy transformation on natural profiles*, Coastal Engineering, 27: 1-20.

19- van Rijn, L.C., Walstra, D.J.R., Grasmeijer, B., Sutherland, J., Pan, S. and Sierra, J.P., (2003), *The*

predictability of cross-shore bed evolution of sandy beaches at the time scale of storms and seasons using process-based profile models, Coastal Engineering, 47(3), pp.295-327.
20- Bijker, E. W. (1968). *Development of a third generation shallow-water wave model with unstructured spatial meshing.* In 11th Coastal Engineering Conference Proceedings, ASCE, 11th Coastal Engineering Conference Proceedings (pp. 415-435).